

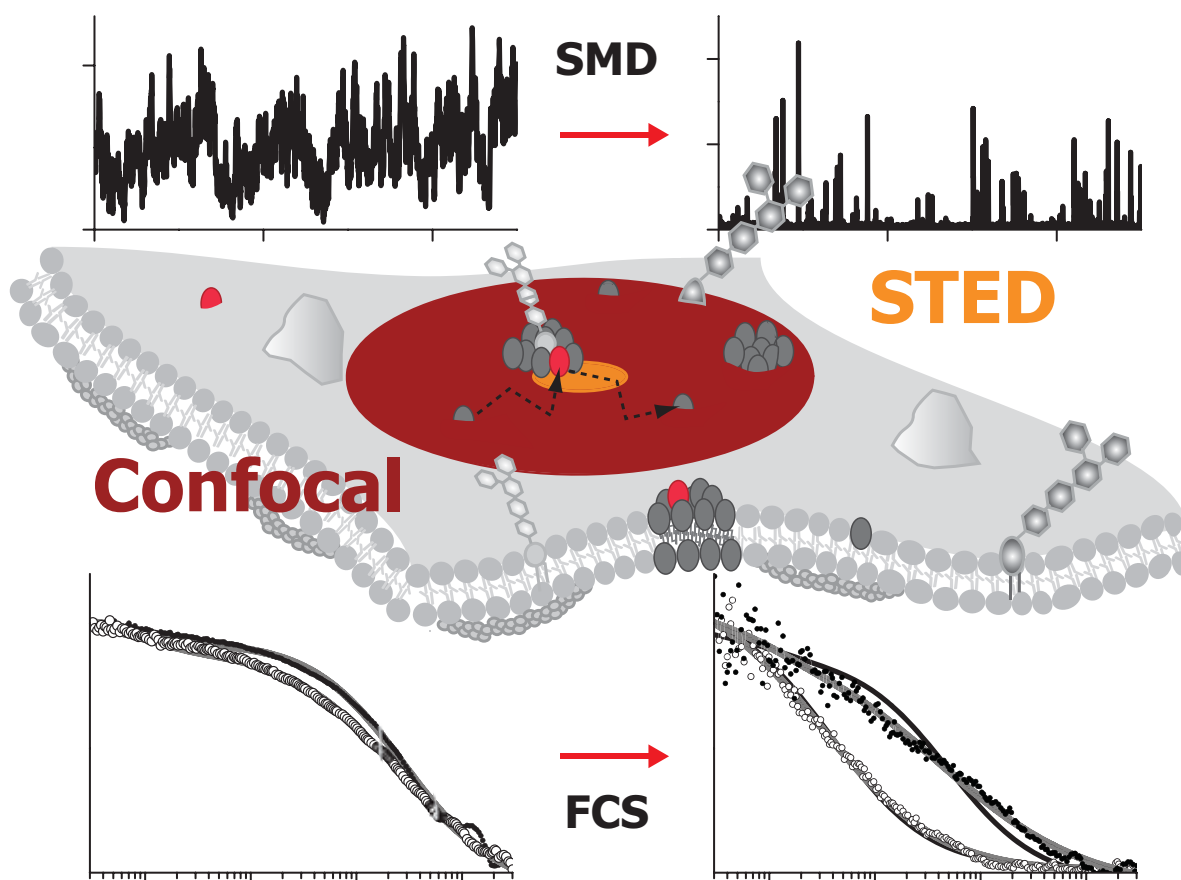
CONFOCAL APPLICATION LETTER

reSOLUTION

A User's Guide to STED-FCS

Stimulated Emission Depletion-Fluorescence Correlation Spectroscopy

Dr. Christian Eggeling, Max Planck Institute for Biophysical Chemistry, Göttingen, Germany and Leica Microsystems



Contents

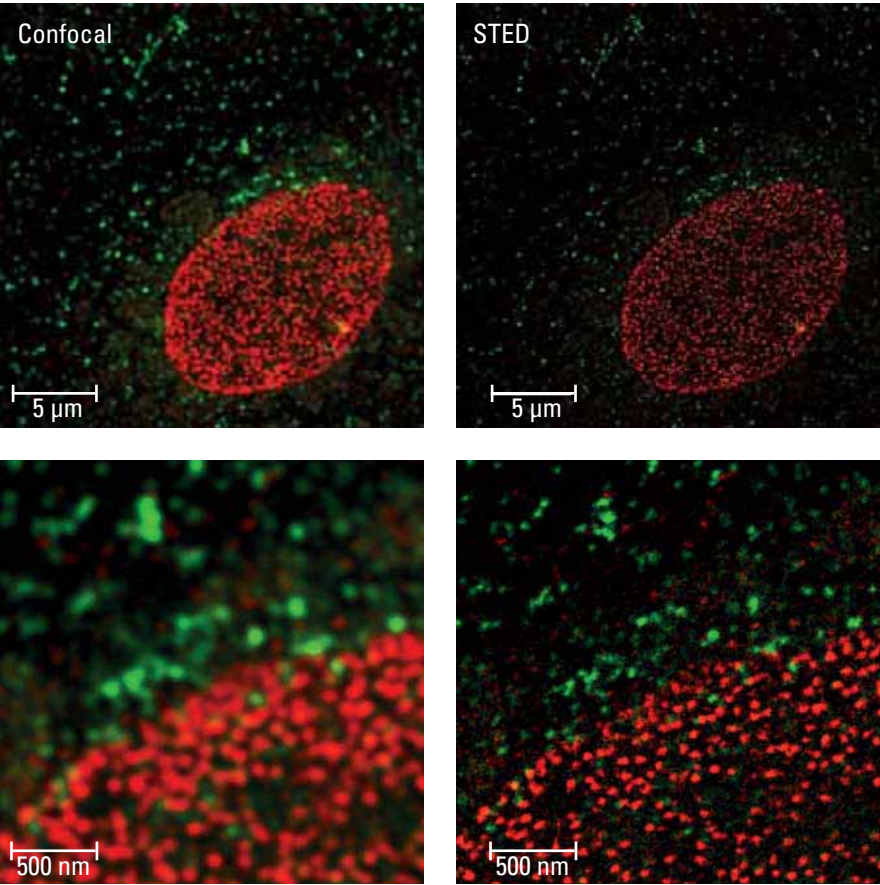
1.	STED-FCS: Introduction	3
2.	STED-FCS: Fitting	4
2.1.	Models	4
2.2.	Calibration	5
2.3.	Sample: Fitting Steps	7
3.	STED-FCS on the Leica Microscope	9
4.	Literature	9
5.	STED-FCS Curve Fitting Using PicoQuant's SymPhoTime Software	10

This application letter is a practical guideline on how to set up and analyze STED-FCS experiments. It consists of two basic parts:

The first part (chapters 1 to 4), written by Christian Eggeling, covers theoretical background and provides essential information on how to plan and set up a STED-FCS experiment. Further, it describes data analysis and discusses the example data.

The second part (chapter 5), by Leica Microsystems, describes data fitting using a Leica TCS STED CW with SMD FCS.

Cover:
Single molecule fluctuations (upper panel) and respective correlation curves (lower panel) of fluorescent lipid analogs diffusing in a supported bilayer. The data were recorded either from a confocal volume (left) or STED volume (right).



Nuclear pore complexes and clathrin coated vesicles of adherent cell stained with BD Horizon V500 (red) and Oregon Green 488 (green), respectively.

1. STED-FCS: Introduction

Fluorescence Correlation Spectroscopy (FCS) is a non-invasive and very sensitive analysis technique, allowing for the disclosure of complex dynamic processes such as diffusion and kinetics. FCS is usually combined with far-field (confocal) microscopy, which allows experiments using living cells. Often however, prominent, biological problems cannot be solved due to the limited resolution (> 200 nm) of conventional optical microscopy. For example, using a conventional optical microscope, FCS requires rather low concentrations of fluorescently-labeled molecules. Sometimes, this can preclude its otherwise very promising application to (endogenous) systems where molecular concentrations of several micro-mol per liter (μM) is required. Further, the limited resolution cannot fully characterize dynamic interactions on the nanoscale, since it cannot directly measure on the relevant spatial scales. Examples are lipid-lipid and lipid-protein interactions such as their transient integration into nanodomains ('rafts'), which are considered to play a functional part in a whole range of membrane-associated processes. The spatial dimension of these domains is supposed to be on molecular scales and the direct, non-invasive observation of them in living cells is thus impeded by the resolution limit.

Using the superior spatial resolution of STimulated Emission Depletion (STED) far-field microscopy with effective observation areas down to 20-30 nm in diameter in living cells [1], FCS can now be applied at rather large fluorophore concentrations (Fig. 1A) [2,3], or it can directly and non-invasively detect nanoscopic anomalous diffusion, such as of single lipid or protein molecules in the plasma membrane of living cells (Fig. 1B) [4]. Combining a (tunable) resolution of down to molecular scales with FCS, new details of molecular membrane dynamics can be obtained. Using STED-FCS it was, for example, shown that sphingolipids or 'raft'-associated proteins, unlike phosphoglycerolipids, were transiently (~ 10 ms) trapped on the nanoscale in cholesterol-mediated molecular complexes [4,5].

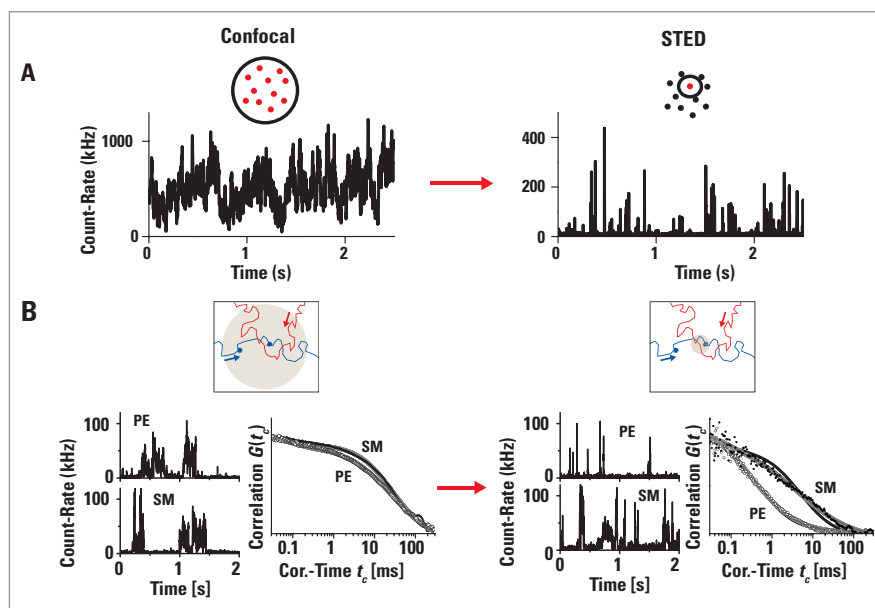


Figure 1: Small observation areas created by STED allow A) the recording of single molecule based fluctuations, i.e., FCS data at much higher concentrations than on a diffraction-limited confocal microscope, and B) the discrimination of free and anomalous diffusion due to interactions on the nanoscale.

A) Detected fluorescence count-rate over time of fluorescent lipid analogs diffusing in a supported membrane bilayer for confocal (left, diameter ~ 240 nm) and STED (right, diameter ~ 50 nm) recordings. At the same concentration of fluorescent lipids, the small observation area of the STED recordings reveals single molecule bursts while the large confocal spot averages over several molecules.

B) Molecular interactions result in an anomalous diffusion of molecules with trapping on the nanoscale (blue track). The small observation area of the STED recordings ensures a significantly reduced transient time of free diffusion and allows distinguishing between free (red track) and hindered diffusion (blue track), while confocal recordings average over these details. Shown are fluorescence count-rate time traces of single-molecule transits and FCS data of a non-interacting fluorescent phospholipid (PE) and an interacting fluorescent sphingolipid (SM) diffusing in the plasma membrane of living cells. Only STED reveals that single-molecule transits of SM are much more heterogeneous than those of PE, also disclosed by a large difference in decay times of the STED-FCS data. In contrast to the confocal FCS data, the STED-FCS data of SM cannot be described by normal free diffusion (black line, right panel), but only by anomalous diffusion (gray line). Confocal recordings would regard diffusion of SM to be slower than PE, but still normal.

2. STED-FCS: Fitting

2.1. Models

STED-FCS data may be analyzed according to common FCS theory, including diffusion and dark (triplet) state dynamics [2-4].

$$G_N(t_c) = DC + G_N(0)G_{Diff}(t_c)G_T(t_c)$$

Here, $G_N(t_c)$ denotes the normalized correlation function with correlation time t_c , DC the offset (usually DC = 1 for normalized correlation data), $G_N(0)$ the amplitude, $G_{Diff}(t_c)$ the diffusion term, and $G_T(t_c)$ the dark state term.

The amplitude $G_N(0) \sim 1/N$ of the FCS data usually scales inversely with the average number N of fluorescent molecules in the detection volume. At constant fluorophore concentration, N scales linearly with the size of the observation volume (or, for two-dimensional data, of the observation area).

Assuming a spatial three- (or two-) dimensional Gaussian profile of the detected fluorescence (observation volume), the diffusion term may be given by

$$G_{Diff}(t_c) = A_1 \left[\left(1 + (t_c / t_{xy,1})^{\alpha_j} \right)^{-1} \left(1 + t_c / t_{z,1} \right)^{-1/2} \right] + \sum_{j=2} A_j \left[\left(1 + (t_c / t_{xy,j})^{\alpha_j} \right)^{-1} \left(1 + t_c / t_{z,j} \right)^{-1/2} \right]$$

$$\text{with } \sum_{j=1} A_j = 1 \quad , \text{ i.e., } A_1 = 1 - \sum_{j=2} A_j$$

$G_{Diff}(t_c)$ may include several ($j = 1, 2, \dots$) differently diffusing components with relative amplitudes A_j , lateral $t_{xy,j} = \text{FWHM}_x^2 / (8D_j \ln 2)$, and axial transit times $t_{z,j} = \text{FWHM}_z^2 / (8D_j \ln 2)$, through the observation volume given by the diffusion coefficient D_j and the lateral and axial full-width-at-half-maximum (FWHM) diameters FWHM_x and FWHM_z of the observation volume, respectively, and the anomalous coefficients α_j . These coefficients are = 1 for free Brownian diffusion and < 1 for anomalous diffusion, e.g., due to obstacles or transient interactions that hinder the diffusion pathway. The contribution of the axial (z) diffusion (i.e. of $t_{z,j}$) on the FCS data is usually much less than of the lateral (x,y) diffusion. Therefore, one can usually neglect anomalous coefficients for $t_{z,j}$. In case of two-dimensional diffusion, such as that of fluorescent lipids or proteins on membranes, the second terms including the axial diffusion $t_{z,j}$ can be neglected, $(1 + t_c / t_{z,j}) = 1$.

The dark state term may be approximated by

$$G_T(t_c) = 1 + \sum_{i=1} T_i / (1 - T_i) \exp(-t_c / \tau_{Ti}) \quad \text{or} \quad G_T(t_c) = 1 - \sum_{i=1} T_i + \sum_{i=1} T_i \exp(-t_c / \tau_{Ti})$$

potentially including several dark states ($i = 1, 2, \dots$) with the average dark state populations T_i and dark state correlation times τ_{Ti} .

Usually STED light features a doughnut-shaped intensity distribution with a central zero along lateral x/y-directions (inset Fig. 2A). Increasing the power P_{STED} of the STED light consequently reduces the observation volume along the lateral directions only, leaving the axial extension unchanged. As a result, the values of t_{xy} decrease, and those of t_z remain unchanged [3]. This user guide will concentrate on this special case.

Experiments have shown so far that STED light does not alter dark state populations [3,4].

N should scale with the observation volume (three-dimensional) or observation area (two-dimensional), and thus decrease with P_{STED} in a similar way as $t_{xy}(P_{\text{STED}})$. This is not true in the case of increasing background contribution – as highlighted below for STED-FCS studies of three-dimensional diffusion.

2.2. Calibration

The calibration of a STED-FCS measurement is the dependence of the lateral diameter $\text{FWHM}(P_{\text{STED}})$ ($= \text{FWHM}_{xy}(P_{\text{STED}})$) of the observation volume on the applied STED power P_{STED} and may be determined from the dependency $t_{xy}(P_{\text{STED}})$ measured for an absolute freely diffusing sample (such as a pure dye in solution, a fluorescent lipid in a one-component model membrane, or a fluorescent lipid freely diffusing in the plasma membrane) [3,4].

- 1) Fit the confocal FCS data with one diffusion component ($j = 1$), no dark state, and $\alpha_1 = 1$ fixed. Float DC , $G_N(0)$, $t_{xy'1}$, and $t_{z'1}$ (the latter is not needed in the case of two-dimensional diffusion; DC may often be fixed). If the fit is bad, add as many dark states i as necessary to describe the data properly (with floating T_i and τ_{Ti}). In some cases it may be appropriate to fix τ_{Ti} to a value approximated from literature (for example the correlation time τ_{Ti} of the triplet state of a usual organic dye in aqueous environment is $\approx 5 \mu\text{s}$).
- 2) Determine $t_{z'1}$, T_i , and τ_{Ti} for the confocal FCS data, and fix their values throughout further analysis ($t_{z'1}$ is not needed in the case of two-dimensional diffusion).
- 3) Fit the FCS data recorded for different P_{STED} with free-floating parameters DC , $G_N(0)$, $t_{xy'1}$, and α_1 . $\alpha_1 = 1$ may also be fixed, since the calibration sample should be characterized by normal diffusion.
- 4) Plot the parameters $t_{xy'1}$ and α_1 against P_{STED} . Values of $t_{xy'1}$ should decrease as indicated in Fig. 2. α_1 should be close to 1 (otherwise check the adjustment of the microscope or the purity of the sample).
- 5) Calculate $\text{FWHM}(P_{\text{STED}})$:
 - $\text{FWHM}(P_{\text{STED}}) = \sqrt{(8D_0 \ln 2 t_{xy'1}(P_{\text{STED}}))}$ if the diffusion coefficient D_0 is known;
 - $\text{FWHM}(P_{\text{STED}}) = \text{FWHM}(0) \sqrt{(t_{xy'1}(P_{\text{STED}})/t_{xy'1}(0))}$ if the confocal diameter $\text{FWHM}(0)$ is known.

For a diffraction-limited spot, $\text{FWHM}(0) \approx 0.6 \lambda/\text{NA}$ may be approximated from the applied wavelength and from the numerical aperture NA of the objective.

A few general things to ensure for STED-FCS measurements:

- Make sure that the calibration $\text{FWHM}(P_{\text{STED}})$ is recorded for the same dye with approximately the same fluorescence lifetime as observed later. Molecular parameters such as fluorescence spectrum or lifetime determine the efficiency and thus, calibration of the STED nanoscope.
- Determine FCS parameters from the average (or median) of at least 5-10 measurements. In living cells, avoid measurement times of more than 10-15 seconds. The probability of detecting rare unrelated events such as diffusing aggregates, vesicles, etc., increases with increasing measurement time.
- The calibration (as done above with values of $t_{xy,1}(P_{\text{STED}})$) may similarly be performed using decreasing values of $N(P_{\text{STED}})$. Due to out-of-axis background (from areas where the STED light is not effective), the signal-to-background ratio of the FCS data of three-dimensional diffusion decreases with increasing P_{STED} , damping the amplitude $G_N(0)$, which results in too large values of N , and thus makes a calibration via $N(P_{\text{STED}})$ infeasible, as shown in Fig. 2A and as in detail discussed in [3].

This damping due to out-of-axis signal is usually not present for recordings on two-dimensional samples such as membranes (unless non-specific background signal from above/below the membrane is present) [3]. However, the signal-to-background ratio often decreases for very large P_{STED} , usually due to fluorescence contributions that are directly excited by the STED light. Therefore, it is recommended to calibrate the STED-FCS experiments with $t_{xy,1}(P_{\text{STED}})$ and not with $N(P_{\text{STED}})$.

- Ensure that the excitation power is low enough – an excitation power that is too high may induce too much photobleaching and thus shorten t_{xy} . This can, for example, be checked by plotting t_{xy} determined from confocal FCS data for different excitation powers.
- Photobleaching by the STED light may result in the lowering of the number of fluorescing molecules in the effective observation volume (since molecules may be photobleached while traversing the STED-doughnut). However, photobleaching by STED has less influence on the transit time t_{xy} . The transit time through the effective observation volume and thus the probability of photobleaching during this transit is significantly shortened for the STED recordings [3,4].
- Usually FCS data recorded for large STED powers is rather noisy, especially for short correlation times t_c . Therefore, it does not make sense to start fitting before $t_c = 1\text{-}5\ \mu\text{s}$ (model membranes, solution) or $t_c = 10\ \mu\text{s}$ (plasma membrane living cell). However, one should use a starting point $t_c = 1\ \mu\text{s}$ for adjustment of dark state parameters on the confocal data (for example, decay of the triplet is usually around $2\text{-}5\ \mu\text{s}$).

2.3. Sample: Fitting Steps

- 1) Fit the confocal data: Start with one diffusion component ($j = 1$), without a dark state, float DC, $G_N(0)$, $t_{xy,1}$, and $t_{z,1}$ (the latter is not needed in the case of two-dimensional diffusion, DC may often be fixed), and fix $\alpha_1 = 1$ (usually the confocal data is not too anomalous). If the fit is bad, add as many dark states i as necessary to properly describe the data (with floating T_i and τ_{Ti}). Fix the determined values of $t_{z,1}$, T_i , and τ_{Ti} throughout further analysis ($t_{z,1}$ is not needed in the case of two-dimensional diffusion).
- 2) Fit the FCS data recorded for different P_{STED} with free-floating parameters DC, $G_N(0)$, $t_{xy,1}$, and α_1 (DC may often be fixed).
- 3) Plot $t_{xy,1}$ and α_1 against $FWHM^2$ (compare Fig. 2C). Normal diffusion is indicated by a linear dependency $t_{xy,1}(FWHM^2)$ and constant values of α_1 , anomalous diffusion by a change of α_1 (specifically a decrease towards small FWHM), and a non-linear dependency of $t_{xy,1}(FWHM^2)$. See references [3-5] for interpreting the dependencies and for further analysis possibilities of the anomalous diffusion (for example, for extracting kinetic parameters of transient trapping).
- 4) One may also calculate the diffusion coefficient $D_1(P_{STED}) = FWHM^2(P_{STED}) / (8 \ln 2 t_{xy,1}(P_{STED}))$ and plot it against FWHM. D_1 should stay constant for free diffusion, decrease toward small FWHM for trapping-like, and increase toward large FWHM for hopping-like diffusion constraints [5].

Comment to 1):

Additional terms may not only result from dark state kinetics, but also from additional diffusing species (such as unbound fluorophore). How to differentiate dark state kinetics from diffusion:

- Continue fitting data by adding dark state terms (floating parameters T_i and τ_{Ti}).
- Values $\tau_{Ti} < 10 \mu s$ usually result from dark state transitions, since diffusion is slower; i.e., such terms can be assigned to dark state kinetics (with parameters T_i and τ_{Ti}).
- Record confocal FCS data for different excitation intensities – dark state kinetics often depend on excitation intensity, i.e., especially T_i should increase with intensity. Therefore, a term definitely describes dark state kinetics if its amplitude T_i strongly depends on the excitation intensity.
- Analyze FCS data with floating dark state parameters for a low STED power also, i.e., for a slightly reduced observation volume, maybe fix T_i to a value known from the confocal fits. Diffusion depends on the size of the observation volume, while dark state kinetics do not, i.e., diffusion is present if τ_{Ti} decreases with STED power.

In the case of positive checks for diffusion:

- Add a diffusion term ($j = 2$) instead of a dark state term. Usually, one can assume this additional component to be diffusing normal (e.g., unbound fluorophore), i.e., fix $\alpha_2 = 1$. Fit the confocal FCS data with floating $t_{xy,1}(0)$, A_2 , and $t_{xy,2}(0)$. Determine the values of the transit times $t_{xy,2}(P_{STED})$ of an additional component for different STED powers, either by

$$t_{xy,2}(P_{STED}) = t_{xy,2}(0) FWHM^2(P_{STED}) / FWHM^2(0)$$

or by

$$t_{xy,2}(P_{STED}) = FWHM^2(P_{STED}) / (8 D_2 \ln 2) \text{ with } D_2 = FWHM^2(0) / (8 \ln 2 t_{xy,2}(0))$$

– Fit FCS data for each P_{STED} with fixed $\alpha_2 = 1$, fixed A_2 (from confocal fit) and fixed, calculated $t_{xy,2}(P_{\text{STED}})$, and float DC, $G_N(0)$, $t_{xy,1}$, and α_1 (DC may often be fixed).

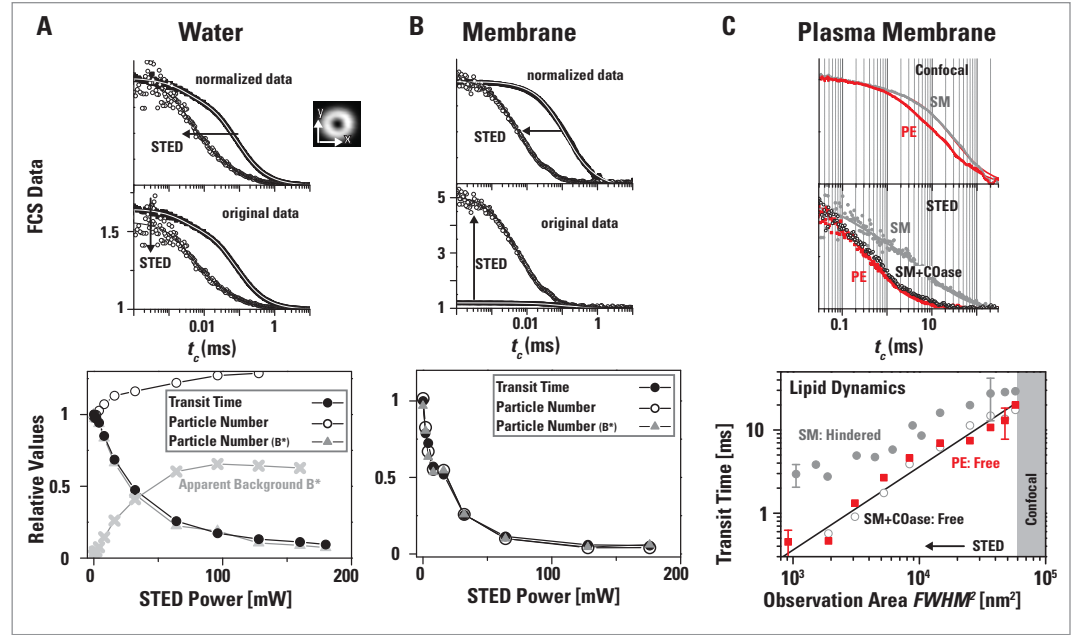


Figure 2: Performance of STED-FCS: Normalized and original STED-FCS data (upper panels) and dependence of transit time $t_{xy,1}$ and particle number N on STED power P_{STED} or observation area FWHM² (lower panels).

- A)** Three-dimensional diffusion of an organic dye in water. While $t_{xy,1}$ (black circles) decreases with P_{STED} as expected, N (open circles) increases due to an apparent out-of-axis background (cross). This bias, however, may be corrected (triangles) [3]. Inset: Doughnut-shaped intensity distribution of the STED focus.
- B)** Two-dimensional diffusion of a fluorescent lipid in a supported membrane. $t_{xy,1}$ (black circles) and N (open circles) decrease with P_{STED} as expected, since no out-of-axis background is present [3].
- C)** Two-dimensional diffusion of fluorescent lipids (PE: phosphoglycerolipid, SM: sphingomyelin, SM+COase: SM after cholesterol depletion by COase treatment) in the plasma membrane of living cells. $t_{xy,1}$ depends linearly on FWHM² for PE or SM+COase (as expected for free diffusion), while this dependency is non-linear for SM due to hindered diffusion [4].

3. STED-FCS on the Leica Microscope

Fig. 2 shows STED-FCS data recorded with the same lasers as supplied by the pulsed Leica STED microscope (pulsed excitation at 635 nm and pulsed STED at 780 nm).

Fig. 3 shows STED-FCS data recorded on the continuous-wave (CW) Leica TCS STED microscope or with the same lasers as supplied by the Leica TCS STED CW microscope (CW or pulsed excitation at 488 nm and CW STED at 592 nm). Starting from diffraction-limited 180–190 nm, the achievable FWHM usually does not get below 80–100 nm due to the characteristics of CW STED-FCS [6], but it is improved by gated STED-FCS [7].

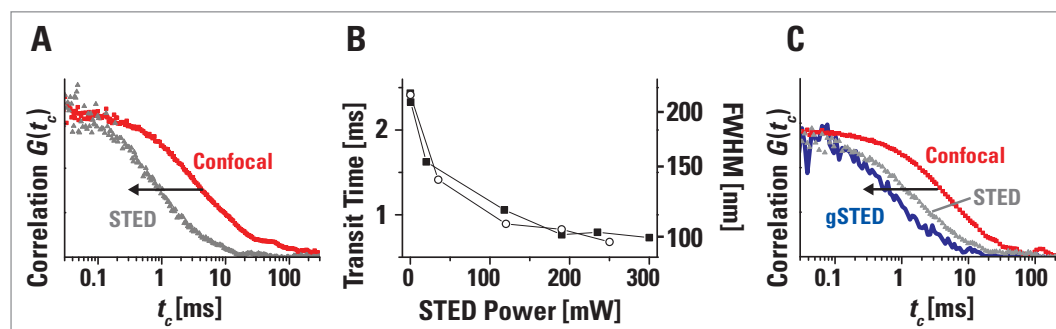


Figure 3: Leica STED-FCS of Bodipy-labeled lipids with CW STED lasers (488 nm excitation, 592 nm STED).

A) Normalized STED-FCS data (red: confocal, gray: STED) recorded on a Leica microscope.

B) Dependence of transit time $t_{xy,1}$ and calculated diameter FWHM of the observation area on CW STED power P_{STED} for two different lipids.

C) Normalized STED-FCS data (red: confocal, gray: STED, blue: gSTED) showing that the resolution of FCS is further increased with gated STED (gSTED) (see [7]). Data in B and C were recorded on a home-built STED nanoscope.

4. Literature

- [1] S.W. Hell. "Far-Field Optical Nanoscopy", *Science*, 316, 1153, (2007).
- [2] L. Kastrup et al. "Fluorescence fluctuation spectroscopy in subdiffraction focal volumes", *Phys. Rev. Lett.*, 94, 178104, (2005).
- [3] C. Ringemann et al. "Exploring single-molecule dynamics with fluorescence nanoscopy", *New J. Physics*, 11, 103054, (2009).
- [4] C. Eggeling et al. "Direct observation of the nanoscale dynamics of membrane lipids in a living cell", *Nature*, 457, 1159, (2009).
- [5] V. Mueller et al. "STED nanoscopy reveals molecular details of cholesterol- and cytoskeleton-modulated lipid interactions in living cells", *Biophys. J.*, 101, 1651, (2011).
- [6] M. Leutenegger et al. "Analytical description of STED microscopy performance", *Opt. Expr.*, 18, 26417, (2010).
- [7] G. Vicidomini et al. "Sharper low power STED nanoscopy by time gating", *Nat. Meth.*, 8, 571 (2011).

5. STED-FCS Curve Fitting Using PicoQuant's SymPhoTime Software

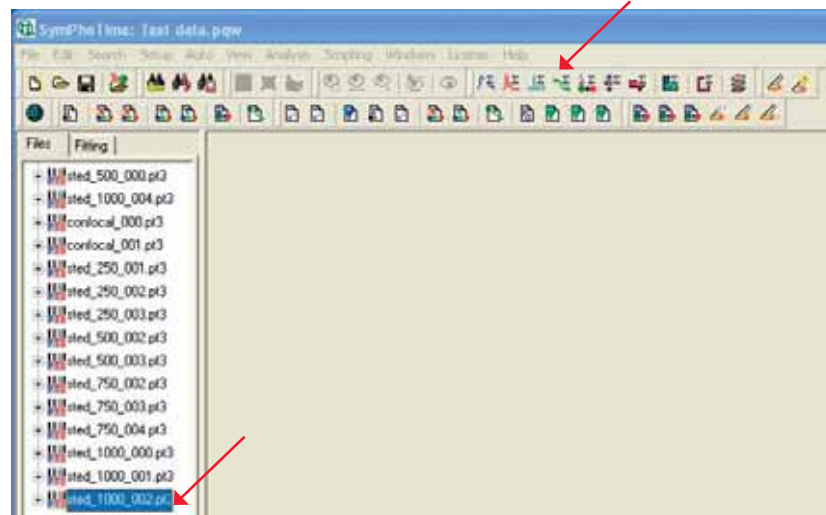
The Leica TCS STED CW system with integrated SMD FCS includes the data analysis software "SymPhoTime" (SPT) from PicoQuant GmbH. For two-dimensional experiments, e.g., for STED-FCS of membrane diffusion, built-in models can be used for data analysis (as described below). For three-dimensional STED-FCS measurements, e.g., in solutions, there is no built-in model in SPT. However, correlation curves can be exported as ASCII files and then analyzed using other programs.

How to fit two-dimensional STED-FCS data into the SPT software – step-by-step:

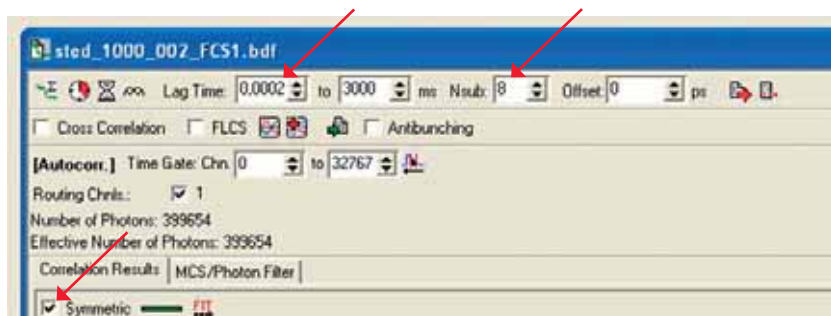
1. Open the workspace containing the raw data or import the raw data into a new workspace.



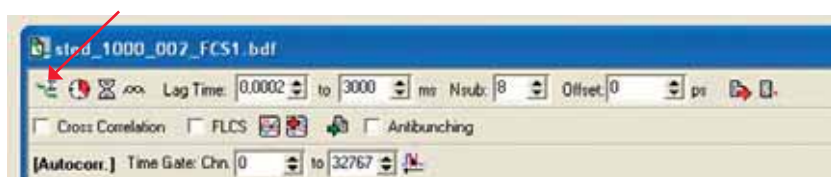
2. Highlight the data set to be processed and calculate its correlation curve using "FCS Trace".



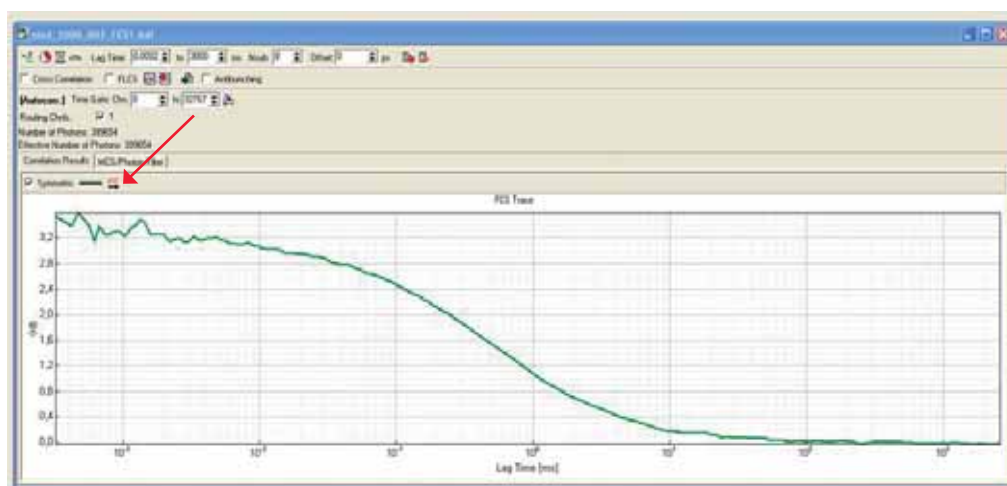
3. Recommended settings: Lag Time: 0.0002, Nsub: 8, Offset: 0, and Symmetric.



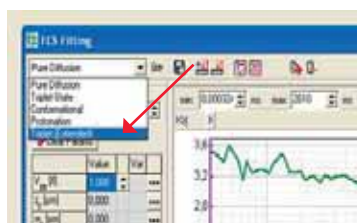
4. Press "Correlate". Now the correlation curve will be calculated and displayed.



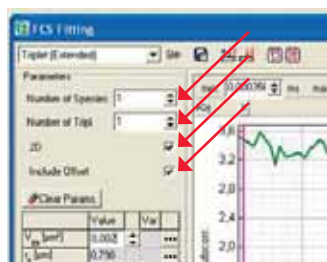
5. Press "Fit".



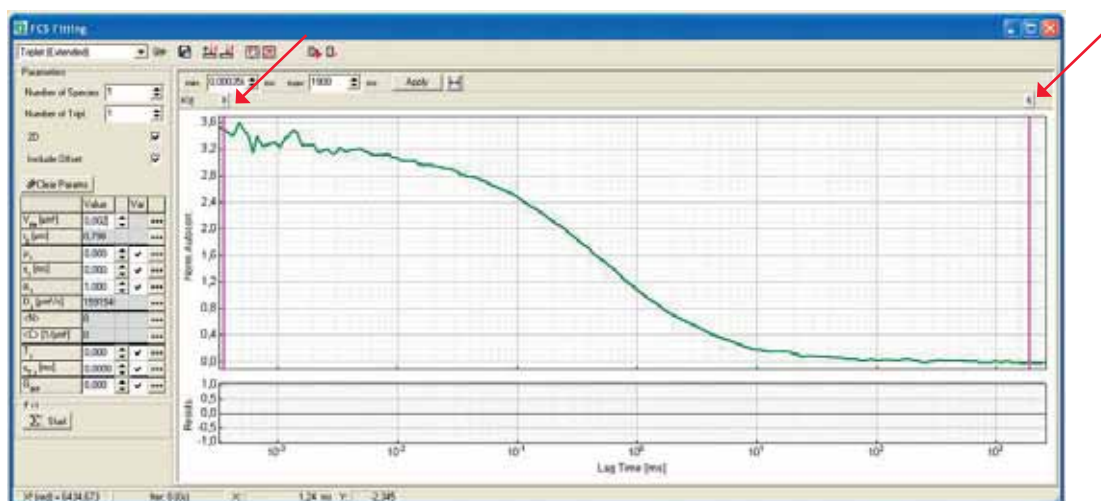
6. Within the fitting dialogue, select the model, "Triplet Extended".



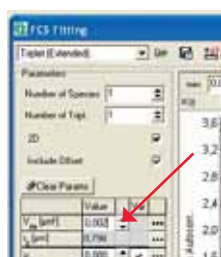
7. Within the fitting dialogue, select the number of fluorescent species (1, 2, 3, or 4, j in Eq. 1), the number of triplet states (1 or 2, i in Eq. 2), check the box "2D". If the correlation curve does not approach the zero line, check the box "Include Offset" as well.



8. Select an appropriate fitting range. For example, start at 1 μ s (for adjustment of dark state parameters on the confocal data), 1-5 μ s (model membranes, solution) or 10 μ s (plasma membrane of living cells) and end at 1000 ms – see comment above.



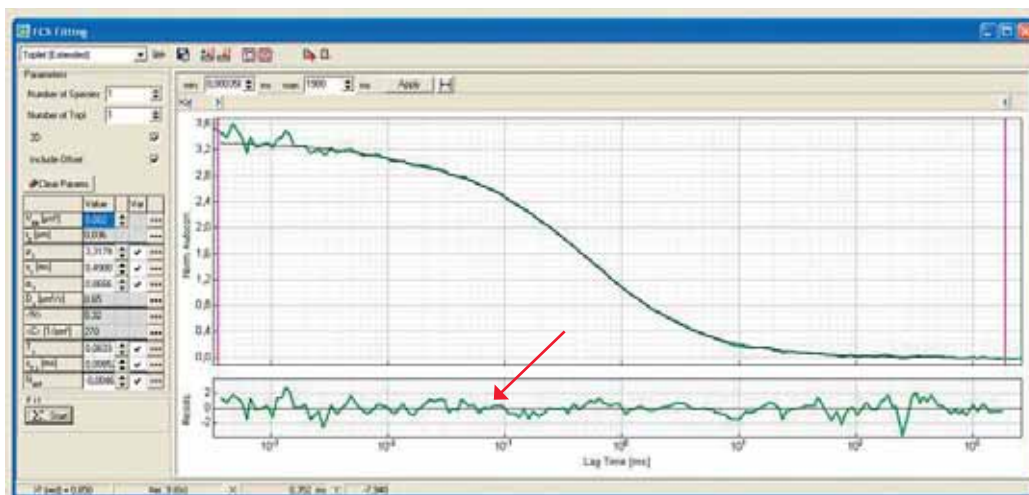
9. If known, specify the effective observation area of V_{Eff2D} . This value is not fitted, but serves only for the calculation of diffusion coefficients, etc.. r_0 indicates the corresponding effective radius at $1/e^2$ intensity ($\text{FWHM} = r_0 \sqrt{8 \ln 2}$, Eq. 1).



10. To start the fitting process, press the "Start" button.



11. If the residual curve is scattering around zero without showing waves (as shown here), the selected fitting model well matches the data. Otherwise, add another dark state or another diffusion time as outlined before.



12. The following parameters can be obtained from the fit:

- a. $\rho_1, \rho_2, \rho_3, \rho_4$ – contribution (amplitude of diffusion term) of the fluorescent species $j = 1, 2, 3$, and 4 (A_j in Eq. 1)
- b. $\tau_1, \tau_2, \tau_3, \tau_4$ – transit times of the fluorescent species $j = 1, 2, 3$, and 4 ($t_{xy,j}$ in Eq. 1)
- c. $\alpha_1, \alpha_2, \alpha_3, \alpha_4$ – anomaly coefficients of the fluorescent species $j = 1, 2, 3$, and 4 (equivalent to α_j in Eq. 1)
- d. D_1, D_2, D_3, D_4 – diffusion coefficients of the fluorescent species $j = 1, 2, 3$, and 4. This value is calculated based on the fitted diffusion times τ_j and on the entered value of V_{Eff2D} :

$$D_j = \frac{V_{\text{Eff2D}}}{2\pi\tau_j}$$

This means it is only valid if the effective observation area is correctly entered. Otherwise, D_j can be calculated according to the procedure outlined in chapter 1.3.

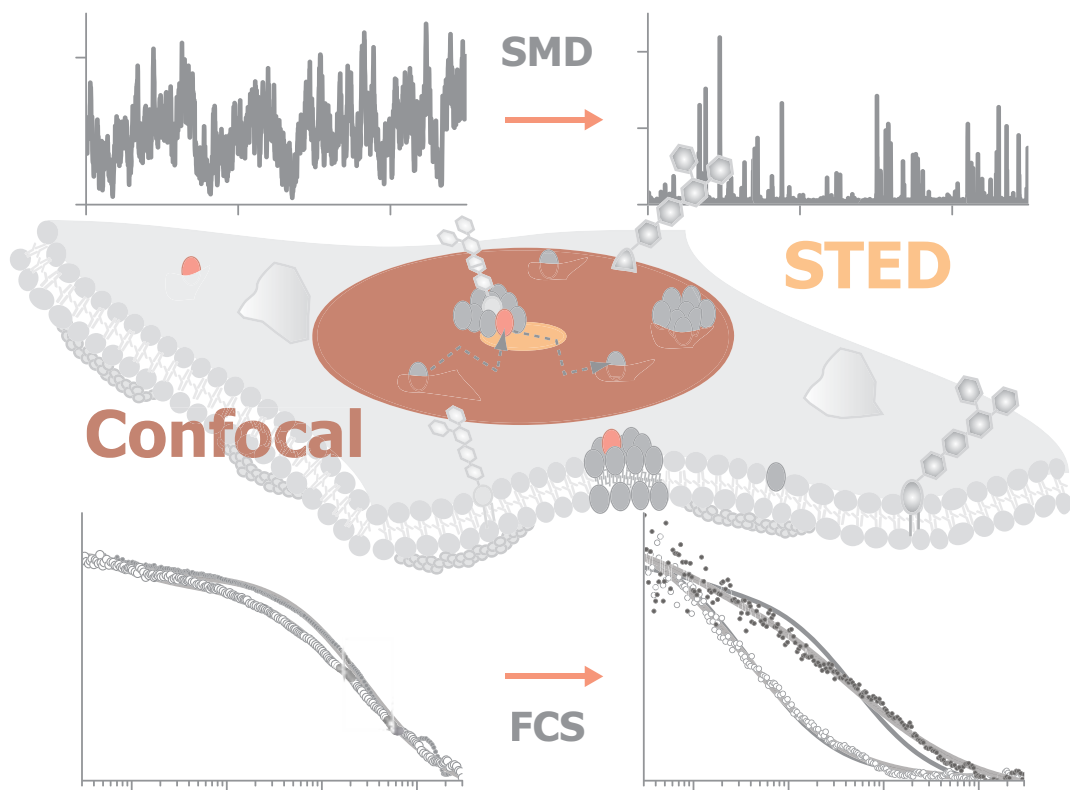
- e. N – total average particle number of all fluorescent species within the observation area. The value is calculated from $G_N(0) = 1/N$ (Eq. 1).
- f. C – total concentration of all fluorescent species within the observation area. This value is calculated based on the values N and V_{Eff2D} . It is correct only if the effective area, V_{Eff2D} , is correctly entered.

$$C = \frac{N}{V_{\text{Eff2D}} N_A} \quad \text{with } N_A - \text{Avogadro constant}$$

- g. T_1, T_2 – fraction of molecules in dark (triplet) state $i = 1, 2$ (T_i in Eq. 2).
- h. τ_{T1}, τ_{T2} – correlation time of the dark (triplet) states $i = 1, 2$ (τ_{Ti} in Eq. 2).
- i. G_{INF} – offset of the correlation curve (DC in Eq. 1).

The fitting procedure described in chapter 5 can be used for two-dimensional experiments for both the system calibration and the data analysis. System calibration requires, a freely diffusing sample in a membrane with a known diffusion coefficient. The diffusion time at different STED laser powers P_{STED} is measured and the corresponding effective volume V_{Eff2D} calculated (see chapter 2.2).

Now, the sample of interest can be analyzed. For each STED laser power P_{STED} the effective volume V_{Eff2D} can be typed into the software and the diffusion time, the anomaly coefficient, and the concentration are automatically derived. Chapter 2.3 gives a detailed description how to continue the analysis of data.



“With the user, for the user”

Leica Microsystems

Leica Microsystems operates globally in four divisions, where we rank with the market leaders.

• Life Science Division

The Leica Microsystems Life Science Division supports the imaging needs of the scientific community with advanced innovation and technical expertise for the visualization, measurement, and analysis of microstructures. Our strong focus on understanding scientific applications puts Leica Microsystems' customers at the leading edge of science.

• Industry Division

The Leica Microsystems Industry Division's focus is to support customers' pursuit of the highest quality end result. Leica Microsystems provide the best and most innovative imaging systems to see, measure, and analyze the microstructures in routine and research industrial applications, materials science, quality control, forensic science investigation, and educational applications.

• Biosystems Division

The Leica Microsystems Biosystems Division brings histopathology labs and researchers the highest-quality, most comprehensive product range. From patient to pathologist, the range includes the ideal product for each histology step and high-productivity workflow solutions for the entire lab. With complete histology systems featuring innovative automation and Novocastra™ reagents, Leica Microsystems creates better patient care through rapid turnaround, diagnostic confidence, and close customer collaboration.

• Medical Division

The Leica Microsystems Medical Division's focus is to partner with and support surgeons and their care of patients with the highest-quality, most innovative surgical microscope technology today and into the future.

The statement by Ernst Leitz in 1907, “with the user, for the user,” describes the fruitful collaboration with end users and driving force of innovation at Leica Microsystems. We have developed five brand values to live up to this tradition: Pioneering, High-end Quality, Team Spirit, Dedication to Science, and Continuous Improvement. For us, living up to these values means: **Living up to Life.**

Active worldwide

Australia:	North Ryde	Tel. +61 2 8870 3500	Fax +61 2 9878 1055
Austria:	Vienna	Tel. +43 1 486 80 50 0	Fax +43 1 486 80 50 30
Belgium:	Groot Bijgaarden	Tel. +32 2 790 98 50	Fax +32 2 790 98 68
Canada:	Concord/Ontario	Tel. +1 800 248 0123	Fax +1 847 236 3009
Denmark:	Ballerup	Tel. +45 4454 0101	Fax +45 4454 0111
France:	Nanterre Cedex	Tel. +33 811 000 664	Fax +33 1 56 05 23 23
Germany:	Wetzlar	Tel. +49 64 41 29 40 00	Fax +49 64 41 29 41 55
Italy:	Milan	Tel. +39 02 574 861	Fax +39 02 574 03392
Japan:	Tokyo	Tel. +81 3 5421 2800	Fax +81 3 5421 2896
Korea:	Seoul	Tel. +82 2 514 65 43	Fax +82 2 514 65 48
Netherlands:	Rijswijk	Tel. +31 70 4132 100	Fax +31 70 4132 109
People's Rep. of China:	Hong Kong	Tel. +852 2564 6699	Fax +852 2564 4163
	Shanghai	Tel. +86 21 6387 6606	Fax +86 21 6387 6698
Portugal:	Lisbon	Tel. +351 21 388 9112	Fax +351 21 385 4668
Singapore		Tel. +65 6779 7823	Fax +65 6773 0628
Spain:	Barcelona	Tel. +34 93 494 95 30	Fax +34 93 494 95 32
Sweden:	Kista	Tel. +46 8 625 45 45	Fax +46 8 625 45 10
Switzerland:	Heerbrugg	Tel. +41 71 726 34 34	Fax +41 71 726 34 44
United Kingdom:	Milton Keynes	Tel. +44 800 298 2344	Fax +44 1908 246312
USA:	Buffalo Grove/Illinois	Tel. +1 800 248 0123	Fax +1 847 236 3009

and representatives in more than 100 countries